Possible mechanism for the room-temperature stabilization of the Ge(111) $T > 300\,^{\circ}C$ phase by Ga

M. Böhringer,* P. Molinàs-Mata, and J. Zegenhagen†
Max-Planck-Institut für Festkörperforschung, Heisenbergstrasse 1, D-70569 Stuttgart, Federal Republic of Germany

G. Falkenberg, L. Seehofer, L. Lottermoser, and R.L. Johnson
II. Institut für Experimentalphysik, Universität Hamburg, Luruper Chaussee 149, D-22761 Hamburg Federal Republic of Germany

R. Feidenhans'l
Risø National Laboratory, DK-4000 Roskilde, Denmark
(Received 7 December 1994; revised manuscript received 27 March 1995)

At low coverages, Ga on Ge(111) induces a hexagonal, domain wall modulated (2×2) adatom phase, stable at room temperature, that is characterized in low energy electron diffraction (LEED) by split $\frac{1}{2}$-order reflections. This pattern closely resembles the one observed for a phase of clean Ge(111) appearing at temperatures above $300\,^{\circ}C$ ($T > 300\,^{\circ}C$ phase). We report scanning tunneling microscopy, LEED, as well as surface x-ray diffraction measurements on the Ga-induced room-temperature (RT) phase and compare it with a model for the $T > 300\,^{\circ}C$ phase of clean Ge(111). RT deposition of Ga yields a metastable $c(2 \times 8)$ structure which upon annealing transforms to the hexagonal (2×2) one. The transition occurs at considerably lower temperatures compared to clean Ge(111) and is irreversible due to pinning of adatom domains at Ga-induced defects, preventing the reordering of the adatoms and the correct stacking of the $c(2 \times 8)$ structure when cooling to RT. For the lowest Ga coverages investigated, a stabilized phase is obtained that resembles a striped (2×2) rather than a hexagonal (2×2) structure. We discuss the possible existence of a striped (2×2) phase as an intermediate state in the transition from the $c(2 \times 8)$ of clean Ge(111) to the $T > 300\,^{\circ}C$ phase. Driven by entropy — and in the presence of Ga by defects — this intermediate phase transforms to a quasihexagonal (2×2) structure above $300\,^{\circ}C$.

I. INTRODUCTION

For the Ge(111)-$c(2 \times 8)$ reconstruction a simple adatom decoration of the truncated (111) surface is generally accepted as a model.[1,2] Compared to the dimer adatom stacking fault structure of Si(111)-(7×7),[3] which requires rearrangement of the substrate atoms to a large extent, the Ge(111)-$c(2 \times 8)$ is a rather "soft" reconstruction, with the adatoms bound relatively weakly to the substrate. In addition, there exist two adatom configurations with only slightly higher energies than the $c(2 \times 8)$: the (2×2) and the $c(4 \times 2)$ reconstructions, differing from the former only in the stacking sequence of adatom rows along $\langle 01\bar{1} \rangle$. In fact, Ge(111)-$c(2 \times 8)$ can be viewed as a regular stacking of (2×2) reconstructed stripes one (2×2) unit cell wide, separated by $c(4 \times 2)$ boundaries.[4]

Together with the softness of the Ge(111)-$c(2 \times 8)$ reconstruction this has several consequences. First, even well prepared Ge(111) surfaces are rich in defects. The main sources of disorder in the $c(2 \times 8)$ structure are small (2×2) or $c(4 \times 2)$ reconstructed domains as well as additional adatom rows along $\langle 01\bar{1} \rangle$ in (2×2) geometry, extending throughout the $c(2 \times 8)$ domains and leading to (2×2) reconstructed stripes broader than one (2×2) unit cell.[4] Second, the clean Ge(111) surface undergoes a phase transition at relatively low temperatures around $300\,^{\circ}C$ to a phase which we call later on the $T > 300\,^{\circ}C$ phase.[5] This phase is characterized in low energy electron diffraction (LEED) by incompletely split, diffuse, 1/2-order reflections. From the observed LEED pattern Phaneuf and Webb[6] proposed a model for the $T > 300\,^{\circ}C$ phase, where (2×2) reconstructed domains are separated by a hexagonal network of $c(4 \times 2)$ reconstructed antiphase domain walls with wall intersections in local $(\sqrt{3} \times \sqrt{3})$ geometry. The ideal, honeycomblike net is disturbed by entropy-driven fluctuations, resulting in a quasihexagonal domain superlattice with no true long range order. Phaneuf and Webb denote this structure as incommensurate (2×2), $I(2 \times 2)$. However, up to now there are no experimental indications for incommensurability of the $T > 300\,^{\circ}C$ phase. Thus we prefer the classification of this structural model as a domain wall modulated (2×2) reconstruction with almost hexagonal symmetry, abbreviated h-(2×2). It is worthy of noting that, apart from the $(\sqrt{3} \times \sqrt{3})$ wall sections, the $c(2 \times 8)$ and the h-(2×2) reconstructions consist of essentially the same structural elements [(2×2) and $c(4 \times 2)$ units], leading to an almost equal density of adatoms and suggesting the charge transfer from adatoms to rest atoms as a common stabilization mechanism.[7] However, the two phases differ drastically in their symmetry due to the $(\sqrt{3} \times \sqrt{3})$

0163-1829/95/52(3)/1948(11)/$06.00

sections in the h-(2×2).

Testing the structure proposed by Phaneuf and Webb for the Ge(111) $T > 300\,^{\circ}\mathrm{C}$ phase by scanning tunneling microscopy (STM) at temperatures above 300 °C may be considered as a challenging task. Although STM at elevated temperatures is possible nowadays, it turns out that above 300 °C the adatoms of the Ge(111) surface are highly mobile, so that within the time scale of a STM experiment no structure can be resolved.[8] However, these studies nevertheless yielded valuable insights into the nature of the transition to the $T > 300\,^{\circ}\mathrm{C}$ phase. Prior to the transition, at temperatures well below $T_c = 300\,^{\circ}\mathrm{C}$, thermally activated concerted shifts of adatoms by one substrate lattice constant in the $\langle 01\bar{1} \rangle$ direction are observed. Furthermore, the transition to the $T > 300\,^{\circ}\mathrm{C}$ phase starts at the domain boundaries of the $c(2 \times 8)$ already below T_c. The area of these "disordered" regions grows continously with temperature [premelting in two dimensions (2D)] until at T_c the entire surface appears disordered. Thus the transition temperature to the $T > 300\,^{\circ}\mathrm{C}$ phase depends on the domain size of the $c(2 \times 8)$structure: the smaller the $c(2 \times 8)$ domains, the lower T_c. Feenstra and co-workers[8] conclude that the transition is essentially first order and becomes continuous only by edge melting due to finite size effects.

In a STM study by Hwang and Golovchenko[9] it was shown that small amounts of Pb decrease the activation energy for the concerted adatom shift via a special mechanism for the creation of T_4 vacancies, which are necessary for the adatoms to move. Consequently, on the Pb-doped surfaces concerted adatom movements occur at much lower temperatures than on the clean Ge(111) surface.

There exists an alternative way to test the structure proposed by Phaneuf and Webb without the need of working with STM at high temperatures. It is known that a variety of elements such as Al,[10] In,[5] Sn,[5] Cu,[11] and Au (Ref. 12) induce a Ge(111) phase stable at room temperature (RT), that exhibits a LEED pattern similar to that of the $T > 300\,^{\circ}\mathrm{C}$ phase of clean Ge(111). A LEED pattern characterized by split 1/2-order spots was also obtained for vicinal Ge(111) surfaces of highly Ga-doped Ge.[13] STM pictures obtained on these surfaces closely resemble the h-(2×2) structure. However, the mechanism of stabilization, especially the individual contribution of misorientation and Ga impurities, was not clear from this investigation.

Here we report results obtained with LEED, STM, and surface x-ray diffraction (SXRD) for annealed Ge(111) surfaces covered with small amounts of Ga. In the range $0.05\ \mathrm{ML} \leq \Theta_{\mathrm{Ga}} \leq 0.25\ \mathrm{ML}$ we observe at RT a LEED pattern characterized by split 1/2-order reflections. We address the following questions:

(i) What is the relation between the Ga-induced RT phase, the $T > 300\,^{\circ}\mathrm{C}$ phase of clean Ge(111), and the h-(2×2) model?

(ii) What is the role of Ga in inducing the RT stabilized phase?

(iii) Do we gain new information from the stabilized phase about the phase transition of clean Ge(111) at 300 °C?

II. EXPERIMENTAL PROCEDURES

The LEED and STM investigations were performed in an UHV system with a base pressure in the low 10^{-10} mbar range. The $c(2 \times 8)$ reconstruction of clean Ge(111) was obtained by repeated Ar sputtering of well-oriented Ge(111) samples (misorientation $< \pm 0.3°$) at 650 °C and $p_{\mathrm{Ar}} \approx 5 \times 10^{-5}$ mbar. Prior to sputtering the sample was cleaned *ex situ* with organic solvents and oxidized in 30% H_2O_2. On surfaces showing an excellent $c(2 \times 8)$ LEED pattern Ga was deposited from a thermal effusion cell at a rate of approximately 1/3 ML per min ($1\ \mathrm{ML} \equiv 7.23 \times 10^{14}\ \mathrm{atoms\,cm^{-2}} \equiv 1.42$ Å Ga) with the sample at RT. The deposition rate was calibrated by a quartz microbalance. Subsequent annealing was monitored by LEED. The STM images were obtained in the constant current mode at ambient temperatures with a commercially available STM.[14] The convention used here is that the bias V_t across the tunnel junction is the voltage of the sample measured with respect to the tip.

The SXRD measurements were performed at the BW2 station at the Hamburg Synchrotron Radiation Laboratory (HASYLAB). Prior to the diffraction measurements the samples were characterized by LEED, reflection high energy electron diffraction (RHEED), and STM. Subsequently the samples were transferred into a portable UHV chamber, which was then mounted on the diffractometer.

III. EXPERIMENTAL RESULTS

A. LEED

Figure 1 gives a sequence of LEED photographs obtained for the clean Ge(111) surface at increasing temperatures. For comparison, Fig. 1(a) shows the well-known LEED pattern of the Ge(111)-$c(2 \times 8)$ surface at RT. Just below the transition to the $T > 300\,^{\circ}\mathrm{C}$ phase [Fig. 1(b)] the 1/8-order reflections disappear; however, there is some intensity extending between the 1/2-order reflections and the nominal positions of the 1/8-order spots. The split 1/2-order reflections are not yet clearly formed. Above T_c [Fig. 1(c)] the splitting of the longitudinally elongated (i.e., elongated in direction of the line connecting the split reflections) 1/2-order reflections is not complete.

After room-temperature deposition of 0.07 ML Ga, LEED shows a $c(2 \times 8)$ diffraction pattern indistinguishable from the pattern of the clean surface within the resolution of our LEED system. When increasing the temperature the surface undergoes a transition which in LEED closely resembles that of the clean surface. However, the transition occurs at considerably lower temperatures ($\Delta T \approx 70$ K for 0.07 ML Ga) and is irreversible, i.e., after cooling the sample to RT the split 1/2-order reflections are still observable. Longer annealing at temperatures between 550 °C and 600 °C yields completely split 1/2-order spots [Fig. 2(a)], which are mainly transversally elongated, i.e., elongated perpendicular to the line

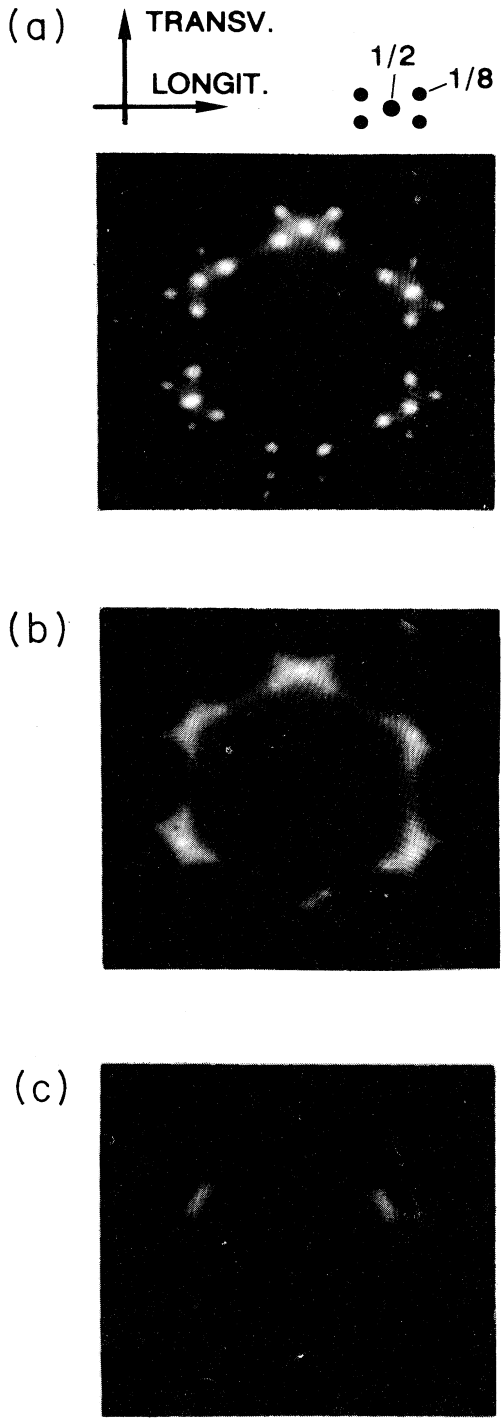

FIG. 1. (a) LEED photograph of the Ge(111)-$c(2 \times 8)$ surface (electron energy $E_0 = 17.0$ eV). (b) LEED photograph of the clean Ge(111) surface just below the transition to the $T > 300\,^{\circ}$C phase ($E_0 = 13.8$ eV). (c) LEED photograph of the Ge(111) surface just above the transition temperature to the $T > 300\,^{\circ}$C phase ($E_0 = 13.6$ eV). In (c) the temperature is ≈ 30 K higher than in (b). In all photographs only reflections around the 1/2-order positions are shown. The longitudinal (longit.) and transverse (transv.) directions are indicated.

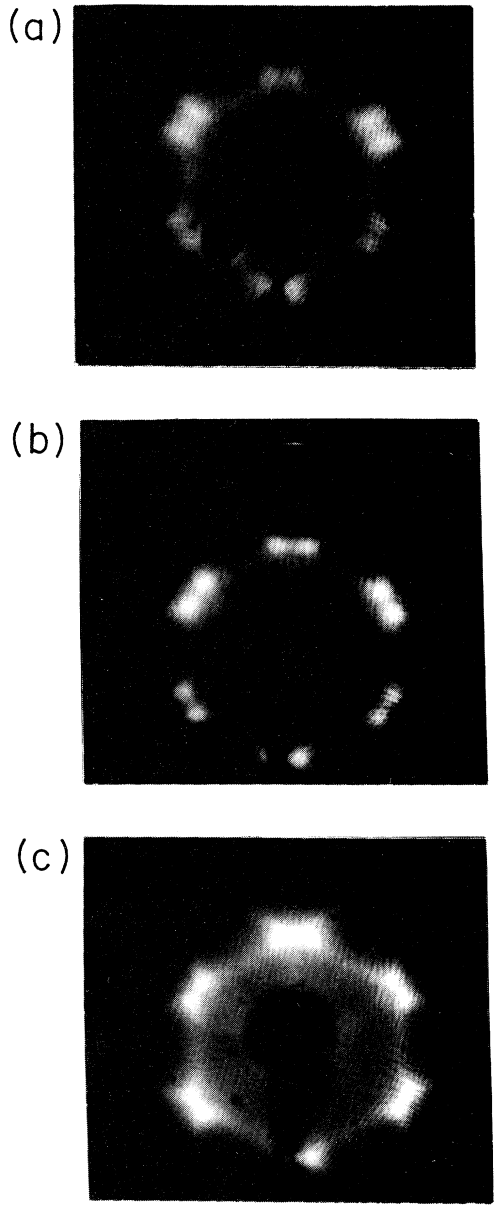

FIG. 2. (a) LEED picture of the Ga-induced RT phase with transversally elongated split 1/2-order reflections ($E_0 = 17.0$ eV). (b) LEED pattern of the Ga-induced RT phase with almost circular split 1/2-order reflections ($E_0 = 16.8$ eV). (c) LEED picture of a stabilized RT phase with intensity mainly between the 1/2-order and 1/8-order positions ($E_0 = 15.4$ eV).

connecting the split spots. Depending on annealing time and annealing temperature the resulting LEED patterns at RT are slightly different, ranging from transversally elongated spots [Fig. 2(a)] over completely split 1/2-order spots with almost circular shape [Fig. 2(b)] to a profile with intensity mainly between the 1/2-order and the 1/8-order positions [Fig. 2(c)]. The series from (a) to (c) can be obtained either by decreasing the amount of Ga de-

posited and keeping constant the annealing parameters or by increasing the annealing time and annealing temperature from (a) to (c) when the same amount of Ga was deposited in each case. Prolonged annealing at 700 – 750 °C finally yields the LEED pattern of the clean $c(2 \times 8)$ reconstructed Ge(111) surface. In the following we will refer to all the RT phases characterized by split 1/2-order reflections as Ga-induced RT phases, irrespective of pronounced differences in the LEED profiles. Nevertheless, these differences are important and will be discussed later.

B. STM

Figure 3(a) shows a small part of an "ideal" boundary between two $c(2 \times 8)$ domains, which both exhibit a regular $c(2 \times 8)$ reconstruction close to the boundary. On a larger scale [Fig. 3(b)] "defects" are visible, i.e., small (2×2) domains in the vicinity of the boundary as well as additional adatom rows along $\langle 01\bar{1} \rangle$ extending from the boundary through the $c(2 \times 8)$ domains [two of these extra rows are also visible in the right part of Fig. 3(a)].

Figure 4 depicts a STM image taken immediately after deposition of 0.05 ML Ga at approximately 50 °C on a $c(2 \times 8)$ reconstructed Ge(111) surface without subsequent annealing. In LEED the typical $c(2 \times 8)$ pattern is still visible. However, STM reveals that the specific stacking of the adatom rows along $\langle 01\bar{1} \rangle$ in the $c(2 \times 8)$ structure is significantly disturbed by an increased number of additional adatom rows leading to stripes in local (2×2) geometry broader than one (2×2) unit cell. In addition, triangular-shaped 2×2 domains, separated by $c(4 \times 2)$ walls with $(\sqrt{3} \times \sqrt{3})$ intersections as well as a high density of other defects are visible. Instabilities in the imaging process when the tip passes over defects with high corrugation may be interpreted as atom exchange between Ga clusters on the surface and the tip, indicating mobile, weakly bound Ga on the surface.

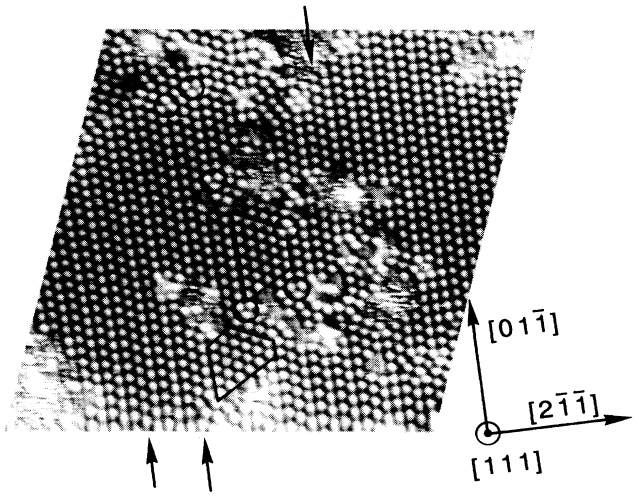

FIG. 4. STM image taken immediately after deposition of 0.05 ML Ga on a Ge(111)-$c(2 \times 8)$ surface at about 50 °C. Additional adatom rows (arrows), adatoms in local $(\sqrt{3} \times \sqrt{3})$ geometry (small circles), and (2×2) domains enclosed in $c(4 \times 2)$ walls (frames) are visible. The large defects with high corrugation are interpreted as Ga clusters (1.0 V, 50 pA, 300 Å × 300 Å).

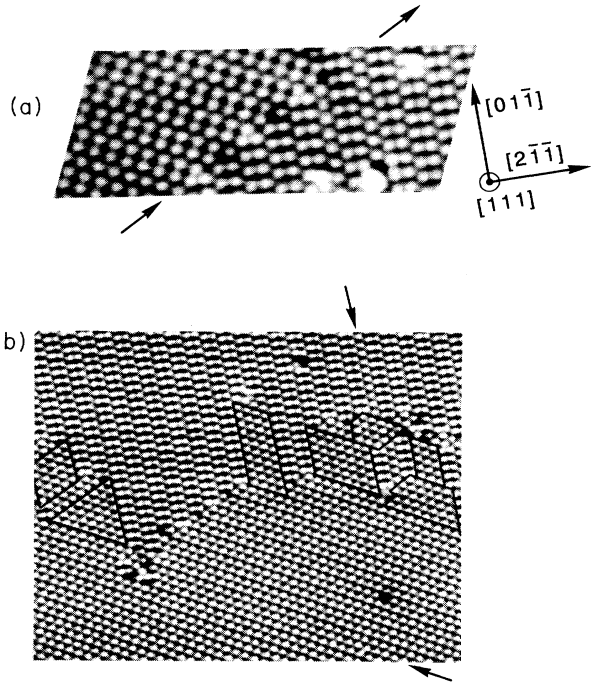

FIG. 3. (a) STM image of the Ge(111)-$c(2 \times 8)$ surface showing an "ideal" boundary between two $c(2 \times 8)$ domains (1.0 V, 50 pA, 180 Å × 70 Å). (b) STM image of the Ge(111)-$c(2 \times 8)$ surface showing locally (2×2) reconstructed areas (marked with a frame) and additional adatom rows along $\langle 01\bar{1} \rangle$ in local (2×2) geometry extending from the boundaries throughout the $c(2 \times 8)$ domains (marked by arrows) (1.0 V, 50 pA, 330 Å × 260 Å).

C. Comparison of the Ga-induced RT phase and the *h*-(2×2) structure

Figure 5 represents a STM image in the dual polarity imaging (DPI) mode on a Ga-stabilized phase prepared by deposition of 0.1 ML Ga and annealing to 550 °C. In the DPI mode the same part of the surface is imaged with opposite polarity of the tunneling voltage by reversing the polarity each time when changing the direction of the scan and storing the data for "forward" and "backward" scan directions separately. By this, occupied (negative bias) and unoccupied (positive bias) surface states can be imaged for exactly the same area.

At RT this surface shows a LEED pattern as depicted in Fig. 2(b). A splitting of the 1/2-order spots is also visible in the power spectrum of the Fourier transform of Fig. 5(a), as shown in Fig. 5(c). At first glance the structure of the Ga-induced RT phase seems to be iden-

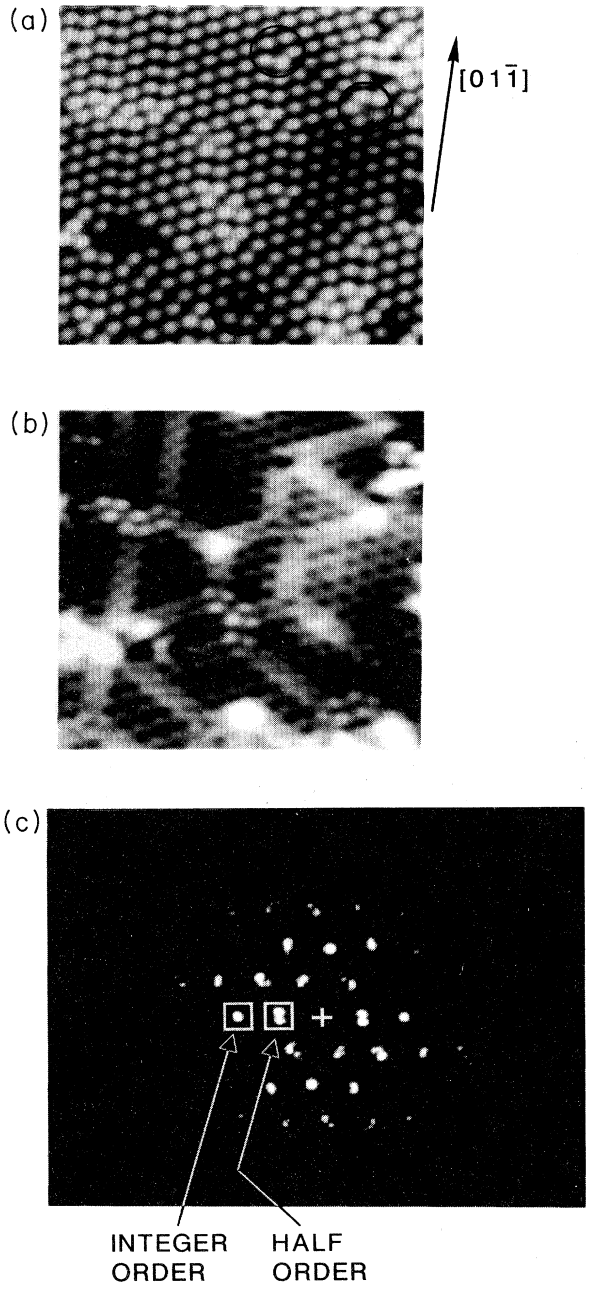

FIG. 5. DPI STM on the Ga-induced RT phase, showing close structural similarity with the h-(2×2) reconstruction: (a) $V_t = 0.6$ V, $I_t = 50$ pA, (b) $V_t = -0.6$ V, $I_g = 50$ pA (150 Å $\times$ 150 Å). (2×2) domains of adatoms are separated by $c(4 \times 2)$ walls with intersections in local $(\sqrt{3} \times \sqrt{3})$ geometry. At positive bias the adatom decoration of the surface is visible, while at negative bias the rest atoms also contribute to the observed corrugation pattern. At negative bias the quasi-hexagonal superstructure is clearly visible due to enhanced contrast at the walls [different charge transfer adatoms-rest atoms for $c(4 \times 2)$ and (2×2) units]. However, a deviation from the ideal h-(2×2) structure is caused by a high density of defects. The circles mark the "minimal" defects mentioned in the text. (c) Power spectrum of the Fourier transform of (a).

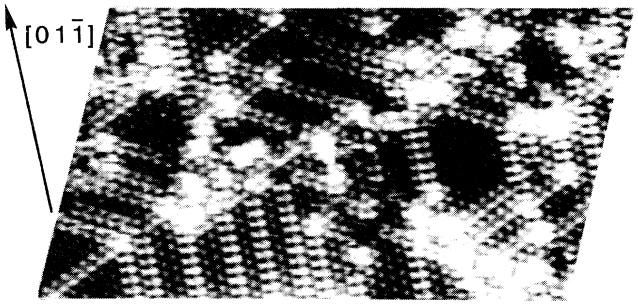

FIG. 6. STM image of a Ga-induced RT phase characterized in LEED [Fig. 2(c)] as transition between the $c(2 \times 8)$ and the h-(2×2) structures. Again, at negative bias the $c(4 \times 2)$ reconstructed walls appear higher than the (2×2) reconstructed stripes (-1.0 V, 50 pA, 330 Å $\times$ 330 Å).

tical with the h-(2×2) structure proposed by Phaneuf and Webb as a model for the $T > 300\,^{\circ}$C phase of clean Ge(111): (2×2) reconstructed domains are separated by an irregular, almost hexagonal net of $c(4 \times 2)$ domain walls with wall intersections in $(\sqrt{3} \times \sqrt{3})$ geometry. As for the Ge(111)-$c(2 \times 8)$, at positive bias only adatoms are imaged with STM. The network of walls is best visible at negative bias, where the $c(4 \times 2)$ walls appear brighter than the (2×2) domains due to different charge transfer from Ge adatoms to Ge rest atoms. Parallelograms made of four adatoms in local $(\sqrt{3} \times \sqrt{3})$ geometry correspond to a $c(4 \times 2)$ domain wall of length zero and therefore can be regarded as regular ingredients of the h-(2×2) structure with fluctuating domain sizes.

However, closer inspection of Fig. 5 reveals differences between the RT phase induced by Ga and the h-(2×2) structure. The former is rich in defects, ranging in size from pentagonal voids with three sides of length $\sqrt{3} \times a_0$ and two sides of length $2 \times a_0$ as minimal defect [Fig. 5(a), $a_0 = 4.0$ Å denoting the substrate lattice constant] to large adatom-free areas. As a consequence, a considerable part of the domain walls ends in voids, leading to domains enclosed by more or less than six $c(4 \times 2)$ reconstructed sides. Thus, we consider the Ga-induced phase to be composed of h-(2×2)-like reconstructed areas and a high density of defects. If we furthermore assume the h-(2×2) structure to be an appropriate model for the $T > 300\,^{\circ}$C phase of clean Ge(111), we can regard the Ga-induced RT phase depicted in Fig. 5 as the RT stabilized $T > 300\,^{\circ}$C phase with a high density of defects. In the following we will refer to this phase as the $T > 300\,^{\circ}$C–Ga phase.

Figure 6 reproduces a STM image at negative tunneling bias obtained on a stabilized RT phase showing the LEED pattern of Fig. 2(c). Again h-(2×2)-like structural elements are visible. However, the image is dominated by another feature: large parts resemble a striped (2×2) phase with $c(4 \times 2)$ domain walls [in short, s-(2×2)].

D. SXRD

Grid scans around the 1/2-order positions failed to identify the split 1/2-order reflections. For an ideal h-

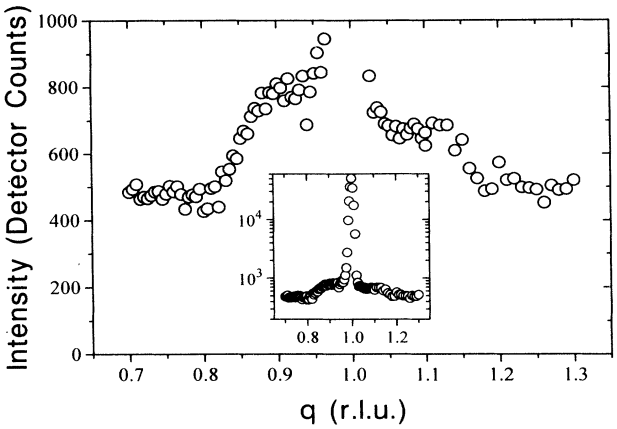

FIG. 7. Result of a SXRD scan around the (1,0) reflection along the ⟨10⟩ direction on a Ga-stabilized RT phase, showing two broad satellites at (0.90,0) and (1.11,0), respectively.

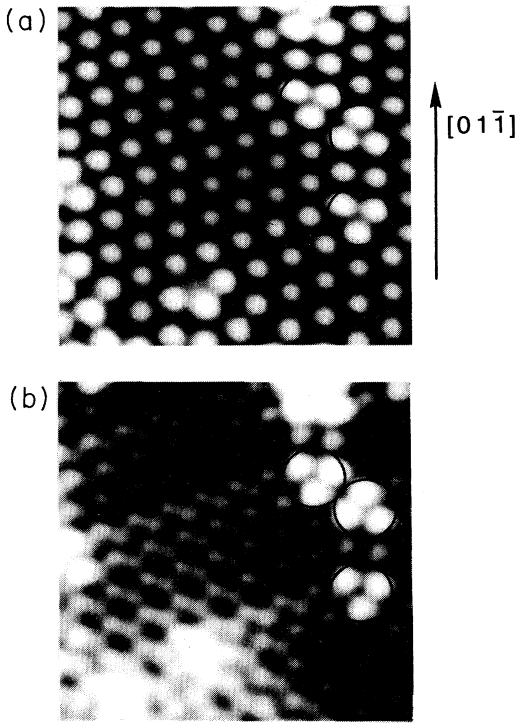

FIG. 8. DPI STM image of the Ga-stabilized phase showing the ($\sqrt{3} \times \sqrt{3}$) reconstructed domain wall intersections (circles) in more detail. (a) positive bias and (b) negative bias (± 1.0 V, 50 pA, 80 Å × 80 Å).

(2×2) reconstruction, these reflections should be strong enough to be observed. However, pronounced disorder in the Ga-induced phase will result in a broadening of the peaks and a decrease in intensity. In Fig. 7 we show a scan around the (1,0) reflection in the (1,0) direction for a Ge(111) sample covered with the $T > 300\,^{\circ}$C–Ga phase. The (1,0) peak is accompanied by two broad side wings at higher $(1 + \delta_+)$ and lower $(1 - \delta_-)q$ values with δ_+ and δ_- approximately 0.10 and 0.11, respectively. We can interpret these as strain-induced features. The broad satellite at (0.9,0) is most pronounced and corresponds to surface areas with approx. 10% increase in the lattice constant, as will be discussed below.

IV. DISCUSSION

A. Does Ga substitute specific positions within the *h*-(2 × 2) structure?

Returning to Fig. 5 and the role of Ga in stabilizing the adatom covered, *h*-(2 × 2)-reconstructed parts of the surface, it is natural to assume that specific positions within this structure are occupied by Ga. For the (2 × 2) and $c(4 \times 2)$ units of the *h*-(2 × 2) structure we assume a Ge adatom decoration as in the $c(2 \times 8)$ and a charge transfer to rest atoms as the stabilization mechanism. Likely sites for a trivalent metal on Ge(111) are the ($\sqrt{3} \times \sqrt{3}$) reconstructed T_4 adatom positions available at the wall intersections of the *h*-(2 × 2). While Ga does not induce a thermodynamically stable ($\sqrt{3} \times \sqrt{3}$) adatom phase on Ge(111) at a coverage of $\approx$ 1/3 ML,[15] the ($\sqrt{3} \times \sqrt{3}$) adatom positions in the *h*-(2 × 2) reconstruction might be regarded as the inital state of a ($\sqrt{3} \times \sqrt{3}$) Ga structure not stable on a larger scale. However, STM results contradict the assumption of Ga in ($\sqrt{3} \times \sqrt{3}$) adatom positions: Fig. 8 shows a DPI image taken on the same surface as Fig. 5. At positive bias the ($\sqrt{3} \times \sqrt{3}$) sections show a slightly higher corrugation compared to the (2 × 2) domains and the $c(4 \times 2)$ walls. At negative bias the STM image is dominated by a strong increase in apparent corrugation at the sites of the ($\sqrt{3} \times \sqrt{3}$) adatoms. This is hard to explain with the assumption of trivalent Ga atoms in these positions, in which case one expects a lower density of occupied states localized at these sites and therefore a lower apparent corrugation at negative bias. On the other hand, the observation can be explained by an altered charge transfer from ($\sqrt{3} \times \sqrt{3}$) Ge adatoms to the surrounding Ge rest atoms compared to the regular charge transfer from $c(4 \times 2)$ and (2 × 2) Ge adatoms [we observe a similar corrugation pattern at ($\sqrt{3} \times \sqrt{3}$) reconstructed defects occurring on the clean Ge(111) surface].

There exists a further, independent argument against Ga in the ($\sqrt{3} \times \sqrt{3}$) positions of the *h*-(2 × 2) reconstructed parts of the $T > 300\,^{\circ}$C–Ga phase. The $T > 300\,^{\circ}$C–Ga phase is observed within a coverage range of 0.05 ML $\leq \Theta_{Ga} \leq$ 0.25 ML. For Ga atoms mainly in ($\sqrt{3} \times \sqrt{3}$) positions of the *h*−(2×2) structure the domain size, i.e., the periodicity of the domain superstructure, and as a consequence the spot splitting in LEED, should be coverage dependent. Considering the ideal honeycomb domain superstructure of the *h*-(2 × 2) and assuming all Ga atoms to occupy ($\sqrt{3} \times \sqrt{3}$) sites one obtains for 0.07 ML Ga coverage a superlattice periodicity of 97 Å and for 0.25 ML Ga [where the domains consist of a single Ge

adatom and the domain walls are one (2×2) unit long] a periodicity of 42 Å. The corresponding variation of the splitting of the 1/2-order spots between 0.04 and 0.1 (in units of the reciprocal lattice mesh) should be clearly detectable in LEED. However, no coverage dependence of the splitting of the 1/2-order spots is visible within the resolution of our LEED system, from which we determine a periodicity of ≈ 40 Å for the domain superlattice of the Ga stabilized phase, i.e., a periodicity corresponding to the minimal size of the (2×2) domains.

With similar arguments from STM and LEED we also exclude substitution of other specific adatom and rest atom positions within the h-(2×2) reconstructed parts of the $T > 300\,^{\circ}$C–Ga phase by Ga atoms. Moreover, from STM at different biases we conclude that Ga does not even occupy sites in the h-(2×2) structure in a random distribution to any significant extent.

B. Ga-induced defects

Summarizing the results from LEED and STM at different biases we deduce that the h-(2×2)-like reconstructed areas of the $T > 300\,^{\circ}$C–Ga phase are mainly composed of Ge T_4 adatoms and Ge rest atoms without any significant amounts of Ga within these areas. To answer the question where the Ga atoms are located within the $T > 300\,^{\circ}$C–Ga phase, we first quote results described in the literature. It is known from STM studies[16] that at coverages below 0.05 ML Ga atoms can substitute rest atom positions within the first substrate layer of an otherwise preserved $c(2\times8)$ reconstruction. Above 0.3 ML coverage an adatom-free discommensurate domain superlattice is formed with Ga atoms substituting all Ge atoms in the first substrate layer.[15,17,18] Extrapolating between these limiting cases we propose that also between 0.05 ML and 0.25 ML after annealing the Ga atoms are located in the substrate surface layer, forming small islands and thus giving rise to the adatom-free defects visible in STM images on the Ga-stabilized phases.

In the SXRD measurement shown in Fig. 7 the broad satellite at (0.90,0) arises from an $\approx 10\%$ increased lattice constant within small surface areas with local (1×1) substitution of surface layer Ge by Ga. The same value of strain is obtained from x-ray standing wave measurements (STM)[17] and (STM)[18] as well as *ab initio* calculations[17] for the discommensurate phase appearing at higher Ga coverages, where the whole surface is covered with a periodic arrangement of (1×1) reconstructed domains. Due to an antiphase scattering condition between adjacent domains the peak at (0.9,0.0) is extinguished and direct evidence for the internal mismatch is missing in the SXRD diffraction pattern of the discommensurate phase.[15,18] For the low coverages discussed here, however, no global superstructure of (1×1) domains is induced by Ga. The patches with local Ga substitution are uncorrelated. Thus the antiphase condition does not hold and the mismatch becomes visible in SXRD. The local Ga substitution does not destroy the underlying Ge(111)-(1×1) structure but merely distorts it. Local expansion of the lattice by Ga must be compensated by a contraction in the vicinity. The peak at higher q value (1.11,0) is the footprint of these areas with decreased lattice constant.

C. The irreversibility of the phase transition in the presence of Ga

We next address the question why the phase transition is irreversible in the presence of Ga and propose that a pinning of (2×2) domains at Ga-induced defects in the substrate surface layer is responsible for the conservation of the h-(2×2)-like structure at RT. In Fig. 9 this pinning is illustrated in a microscopic model. Defects in the substrate surface give rise to drastic local changes in the surface potential, favoring one of the possible (2×2) domain types. They prevent the reordering of the adatom rows along $\langle 01\bar{1}\rangle$ to the specific stacking of the $c(2 \times 8)$ reconstruction and preserve the surface in a state that according to the STM images corresponds to a h-(2×2) reconstruction with a high density of defects (Fig. 5) or to a structure between a striped and a hexagonal (2×2) (Fig. 6). This scenario is further supported by the observation that at temperatures above 300 °C in LEED the shape of the split spots of the Ga-stabilized phase is preserved and does not change to the longitudinally elongated reflections typical for the $T > 300\,^{\circ}$C phase of clean Ge(111). Once the (2×2) domains are pinned at defects they remain pinned even for temperatures above T_c of the clean surface.

The different direction of elongation of the split 1/2-order reflections for the Ga-stabilized phase and the $T > 300\,^{\circ}$C phase may be explained by the large defect density in the former. For the h-(2×2) on an ideal hexagonal substrate without defects the succession of the four types of (2×2) domains along a certain direction on the surface is determined by the $c(4 \times 2)$ antiphase domain boundaries separating the domains. The fluctuation in domain size does not alter this succession and results in a longitudinal elongation of the split spots. At high defect concentration, however, the succession of the defect pinned domains along a certain direction is more arbitrary. Thus the coherence in the succession of the domains is disturbed, resulting in transversally elongated split reflections.

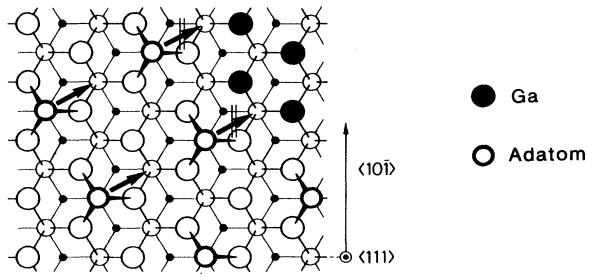

FIG. 9. Microscopic model for the pinning of domains at defects caused by substitutional Ga in the first substrate layer. At the positions of the Ga atoms no dangling bonds are available and the adatoms cannot bind.

The proposed model of pinning at defects also explains some related experimental observations.

(i) As mentioned in the Introduction a great variety of other elements are known to induce at low coverages a RT phase with a LEED pattern similar to that of the $T > 300\,^{\circ}\mathrm{C}$ phase. It is hard to imagine, for example, substitution of specific sites within the h-(2×2) reconstructed areas as the stabilization mechanism common to all these metals. However, all these elements can act as defect-inducing impurities.

(ii) h-(2×2)-like features are often observed near steps or domain boundaries of the $c(2 \times 8)$ of clean Ge(111). These kinds of "defects" might act as pinning centers similar to the Ga-induced defects.

(iii) Finally, the model explains the observation of a h-(2×2)-like structure on misoriented, highly Ga-doped Ge(111) at RT: steps act as additional pinning centers so that a Ga coverage considerably lower than 0.05 ML is sufficient for stabilizations. For the well-oriented Ge(111) surfaces investigated here a higher Ga coverage ($\geq$ 0.5 ML) is necessary to obtain the stabilized phase.

The mechanism of pinning at defects can also provide an explanation for more detailed features of the observed structures. In Fig. 6, where parts of the surface resemble a s-(2×2), the widest (2×2) stripes involve two extra rows of adatoms in (2×2) geometry; broader stripes appear to be unstable and undergo a transition to the hexagonal h-(2×2). To explain the instability of the striped relative to the hexagonal phase we refer to arguments put forward by Villain[19] in the context of commensurate-incommensurate (CI) transitions. Generally at $T = 0$ a striped phase on an ideal hexagonal substrate is preferred relative to a phase with hexagonal symmetry if wall intersections yield a positive contribution to the surface energy. It is reasonable to assume that the $(\sqrt{3} \times \sqrt{3})$ reconstructed domain wall intersections are energetically unfavorable for a h-(2×2) Ge adatom phase [for the Si(111) surface it was shown by Meade and Vanderbilt[20] that a (2×2) structure is slightly lower in energy than a $(\sqrt{3} \times \sqrt{3})$]. However, two reasons may cause a hexagonal phase despite energetically unfavorable wall intersections.

First, the entropy of a hexagonal phase is much larger than the entropy of a striped phase. This argument is discussed in more detail below in connection with the dynamics of the phase transition. Second, the striped phase can be destabilized by an increasing density of defects. This is explained qualitatively in Fig. 10. In (a) a single defect yields a surface potential that locally favors a disturbed stacking of the adatom rows of the $c(2 \times 8)$, i.e., additional rows in local (2×2) geometry. With increasing defect density the probability increases that a second defect falls into the same stripe, which may favor a different registry of the rows. Thus the gain in energy at one defect site is canceled by an energy loss at the other defect. In this case it is energetically more favorable to transform to an irregular hexagonal phase, where the defect pinned domains can arrange in such a manner that there is a net energy gain. This dependence of the detailed surface structure on the local defect density is apparent in the STM image Fig. 11, where in the lower right part with low defect density a s-(2×2) reconstruction is visible, while in the upper left part with a higher local density of defects a quasihexagonal h-(2×2) is formed. An even higher defect density finally results in a complete loss of the coherence in the ordering of the domains (upper right part of Fig. 11). A similar argument

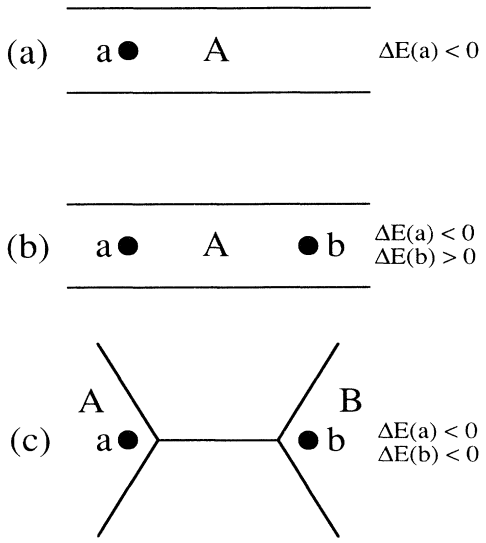

FIG. 10. Model for the defect induced transition from a striped phase to a hexagonal phase on increasing the density of defects. (a) Defect a is locally favoring the (2×2) domain type A. (b) On increasing the defect density a second defect b, favoring a different domain type B, may fall into the same striped domain A. Thus in the domain A the gain in energy at defect a is canceled by the loss in energy at defect b. (c) In the (2×2) phase with hexagonal symmetry the domains and boundaries can arrange in such a way that there is a net gain in energy due to the defects. A similar argument accounts for the destabilization of the (2×2) stripes with increasing width.

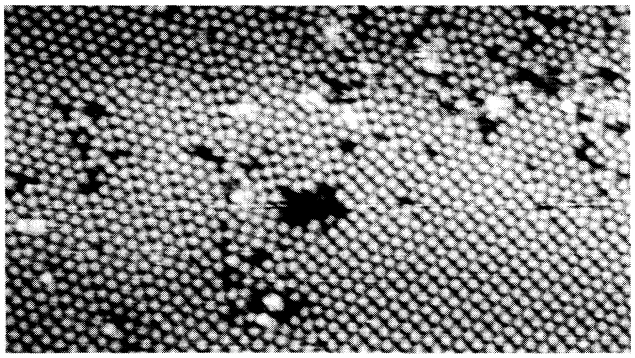

FIG. 11. STM image of a RT phase showing a striped (2×2) reconstruction in regions with low defect density (lower right) and a h-(2×2)-like reconstruction in regions with high defect density (left part). In this case, the defects are induced by small amounts of In, for which, however, we propose the same stabilization mechanism as for Ga (1.0 V, 50 pA, 350 Å $\times$ 220 Å).

essentially applies for the destabilization of the (2×2) stripes with increasing width.

D. Decrease of the transition temperature in the presence of Ga

The assumption of adatom pinning at Ga-induced defects at first sight seems to contradict the decrease of the transition temperature to the h-(2×2) structure after Ga deposition on the Ge(111)-$c(2 \times 8)$. However, we state that without annealing Ga causes disorder/defects mainly within the adatom layer of a metastable $c(2 \times 8)$ (Fig. 4). Only on increasing the temperature to values near the transition temperature does Ga become immobile in the first substrate layer and creates pinning centers. Based on this interpretation we reformulate one of our initial questions: What is the role of (Ga- or otherwise induced) defects in the adatom layer for the decrease in the transition temperature to the $T > 300\,^{\circ}\mathrm{C}$ phase?

As mentioned in the Introduction, STM studies at elevated temperatures proved the transition from the clean Ge(111)-$c(2 \times 8)$ to the $T > 300\,^{\circ}\mathrm{C}$ phase to be an example of premelting in 2D with the transition temperature depending on the $c(2 \times 8)$ domain size.[8] Impurity induced defects decrease the domain size and hence the transition temperature to the $T > 300\,^{\circ}\mathrm{C}$ phase.

Molecular dynamics studies by Takeuchi *et al.*[21] establish that the defect-free Ge(111) surface disorders at $\approx$ 300 °C by correlated diffusion of the adatoms along $\langle 01\bar{1} \rangle$, which represents the structural excitation with the lowest activation energy. This anisotropic diffusion is a result of the bonding topology of the $c(2 \times 8)$. In the absence of defects it has to proceed via intermediate occupation of H_3 positions by Ge adatoms. Defects in the T_4 adatom decoration of the $c(2 \times 8)$, however, allow a direct transition of T_4 adatoms to neighboring T_4 vacancies.[9] We propose that the decrease of T_c by defects in the adatom layer of the $c(2 \times 8)$ structure is the result of a decreased activation energy for concerted adatom shifts if T_4 vacancies are available. Figure 4, which is taken after deposition of small amounts of Ga on a Ge(111)-$c(2 \times 8)$ surface at 50 °C without further annealing, shows this increased number of defects in the adatom layer of the surface. Extra adatom rows in local (2×2) geometry as well as typical features of the h-(2×2) structure indicate that in the presence of Ga adatom movement can already occur at temperatures well below 300 °C.

Figure 12 represents an idealized model for concerted adatom row shifts originating at a $c(2 \times 8)$ domain boundary when increasing the temperature. The structure of the domain wall corresponds to the domain wall visible in Fig. 3(a). For semi-infinite domains semi-infinite adatom rows have to move. If additional — e.g., Ga-induced — defects are present in the adatom layer, the shift of adatom rows starts/terminates at these defects, resulting in a decreased length of the shifted rows.

In this model the transition to the h-(2×2) structure proceeds via an intermediate striped (2×2) structure. The role of Ga in the transition is restricted to the creation of adatom layer defects facilitating concerted

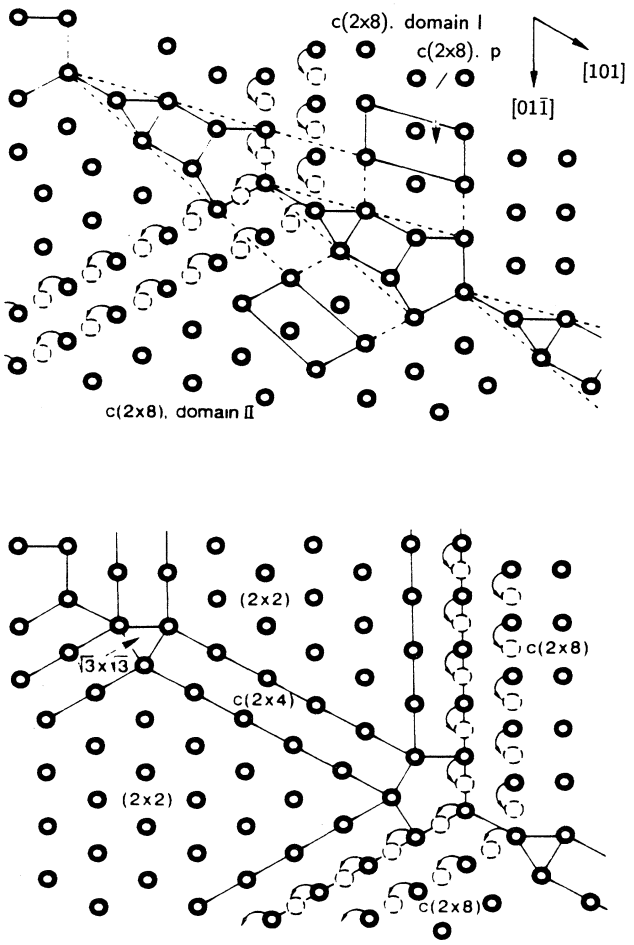

FIG. 12. Model for the origin of the striped (2×2) phase at a domain boundary of the $c(2 \times 8)$ surface via concerted adatom motion. (a) Domain boundary corresponding to STM Fig. 1(a). (b) Concerted movement of adatom rows leads to (2×2) reconstructed stripes.

adatom row shifts. These defects do not necessarily have to be created by impurities such as Ga. They are also present on the "clean" Ge(111) surface (Fig. 3) and the model presented in Fig. 12 might also hold for the initial state of the phase transition to the $T > 300\,^{\circ}\mathrm{C}$ phase of clean Ge(111). So the question arises: Is there any experimental indication for the existence of an intermediate striped (2×2) phase during the phase transition of clean Ge(111)?

E. Does an intermediate striped phase exist in the phase transition of clean Ge(111)?

In Fig. 13(a) we consider the $c(2 \times 8)$ and the (2×2) reconstructions as periodic limiting cases of a striped (2×2) phase with $c(4 \times 2)$ domain walls, i.e., we regard the $c(2 \times 8)$ as a striped phase with unit cell width of the (2×2) domains and the (2×2) as a "striped" phase with infinite width of the domains. The disturbance of the

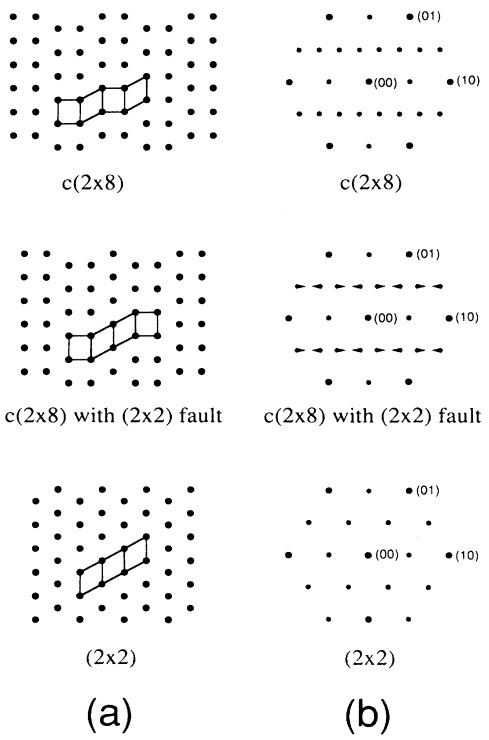

FIG. 13. (a) The $c(2\times 8)$ and the (2×2) reconstructions as periodic limits of a striped (2×2) phase (single domain). (b) LEED patterns corresponding to the structures in (a). The weak 1/4-order reflections of the $c(2\times 8)$ are not shown.

long range order of the $c(2\times 8)$ structure by extra adatom rows in (2×2) geometry results in a displacement of the 1/8-order reflections away from there nominal positions towards the 1/2-order reflections [Fig. 13(b)]. For a simplified model Feidenhans'l *et al.*[2] calculated the structure factor G_{hk} of these reflections to be

$$G_{hk}=\frac{1+ce^{2\pi i(2h+k)}}{1+pe^{2\pi i(2h+k)}+(1-p)e^{4\pi i(2h+k)}} \qquad (1)$$

with p denoting the probability for a (2×2) fault following a regular (2×2) unit cell of the $c(2\times 8)$ structure and with $c=p(1-p)/(2-p)$. The intensity distribution is given by

$$I_{hk}=2\mathrm{Re}(G_{hk})-1. \qquad (2)$$

In Fig. 14 the intensity profile is plotted for $p=0.3$, a value that is obtained by using Fig. 6 as a clue. This profile has to be compared with the LEED pattern shown in Fig. 1(b) for the clean Ge(111) surface immediately below the transition to the $T>300°$ C phase. Clearly, a solely qualitative comparison of the intensity profile obtained from the single-phase structure factor (1) and the LEED pattern Fig. 1(b) is not sufficient for the undoubted proof of an intermediate s-(2×2) phase. Without more quantitative analysis of the spot profile it is difficult to distinguish between the intensity distribution obtained for a s-(2×2) and a simple superposition of h-(2×2) and $c(2\times 8)$ reflections. Precise quantitive LEED spot pro-

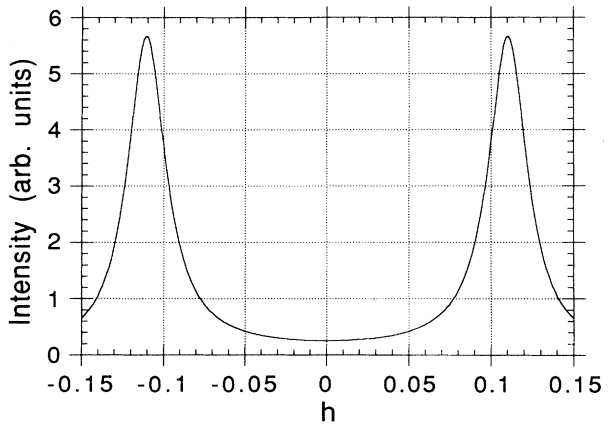

FIG. 14. Intensity profile of the shifted $(\pm 1/8, 1/2)$ reflections according to Eqs. (1) and (2) for $p=0.3$ [cf. Fig. 1(b)].

file analysis or SXRD measurements near the transition temperature are necessary to decide this question. Nevertheless, not only the plausibility of the model presented above points in the direction of an intermediate s-(2×2). Moreover, we tentatively interpret the dynamical change of the LEED pattern obtained on clean Ge(111) near T_c as an experimental hint towards an intermediate s-(2×2). So we are left with the question: Why does the intermediate striped s-(2×2) phase transform to the h-(2×2) with hexagonal symmetry?

F. Transition from the intermediate striped (2×2) phase to the h-(2×2) structure

In the model of Fig. 12 a continued shift of further adatom rows would finally yield two semi-infinite (2×2) domains separated by one $c(4\times 2)$ domain wall. Obviously this does not happen in the case of the real surface. To explain the instability of the striped phase above T_c we again refer to Ref. 19. It was already mentioned above that at $T=0$ a striped domain wall modulated structure is formed on a defect-free hexagonal substrate if wall intersections are energetically unfavorable. However, at $T>0$ the minimum of the free energy $F=U-TS$ determines the structure. A regular hexagonal honeycomb network can be transformed to a more irregular structure simply by changing the lengths of the sides of the hexagons while keeping constant the total length of the walls and the total number of wall sections. Neglecting the weak wall-wall interaction, this transformation does not change the energy of the hexagonal phase. Each of these "breathing" modes represents a soft degree of freedom contributing to the entropy. Thus a hexagonal phase has a much higher entropy than a striped phase and at high temperatures the transition from the striped to the hexagonal phase can be entropy driven. This argument should especially hold for the destabilization of an intermediate striped phase in the phase transition of clean Ge(111). At temperatures around 300 °C, where the adatoms are in fast movement, the entropy term in the free energy dominates the free energy and

effects the transition from the striped to the hexagonal phase. For the Ga-decorated surface the second destabilization mechanism already mentioned above — the pinning of adatom domains at defects — may also play an important role in the dynamics of the transition from the metastable $c(2 \times 8)$ via an intermediate striped phase to the h-(2×2), when at increasing temperatures more and more Ga is immobilized in the substrate surface layer.

G. Comparison with a lattice gas model

The transition of clean Ge(111) to the $T > 300\,^{\circ}\mathrm{C}$ phase was investigated in a Monte Carlo simulation of a lattice gas model by Sakamoto and Kanamori.[22] The adatoms were represented by pairwise interacting particles on a triangular net. Direct neighbors (distance a_0) were excluded and the interaction energy V_2 of second neighbors (distance $\sqrt{3} \times a_0$) chosen positive to avoid a $(\sqrt{3} \times \sqrt{3})$ ground state. Depending on the ratio V_3/V_2 a (2×2) or $c(4 \times 2)$ reconstruction was obtained as ground state; the $c(2 \times 8)$ was stabilized by inclusion of a repulsive sixth neighbor interaction $V_6 > 0$. In all ground states no adatom triplets of mutually second neighboring particles appeared, corresponding to the three adatoms with mutual $\sqrt{3} \times a_0$ distance that form the walls intersections in the h-(2×2) structure. However, on increasing the temperature, these triplets begin to form. In fact, the entropy of the system can be approximated by a universal function of the number of triplets and the presence of the triplets is essential for the entropy gain required for the transition to the $T > 300\,^{\circ}\mathrm{C}$ phase. Above the transition temperature the gain in entropy renders the free energy of the vertices negative — in accordance with the arguments of Villain. The phase appearing above T_c is characterized by small size (2×2) domains, separated by a network of $c(4 \times 2)$ walls which intersect in the triplets or in voids (defects). Snapshots of the particle arrangement just above the transition temperature closely resemble the adatom arrangement in Fig. 5. The smallest voids appearing in the lattice gas model correspond to the minimal defects in Fig. 5.

V. SUMMARY

We conclude that the conservation at RT of a hexagonal, domain wall modulated (2×2) adatom reconstruction on annealed, Ga-decorated Ge(111) surfaces is effected by domain pinning at Ga-induced defects in the substrate surface layer. The observed reconstruction is closely related to a h-(2×2) model of the $T > 300\,^{\circ}\mathrm{C}$ phase appearing on clean Ge(111) at temperatures above $300\,^{\circ}\mathrm{C}$. The detailed structure of the stabilized phase depends on the local density of defects. Without annealing Ga causes defects mainly in the adatom layer. These defects decrease the transition temperature to the h-(2×2) phase by decreasing the activation energy of concerted adatom movement. In a model we tentatively propose that the transition from the $c(2 \times 8)$ to the $T > 300\,^{\circ}\mathrm{C}$ phase proceeds via an intermediate striped (2×2) phase for the clean as well as for the Ga-covered surface. This intermediate striped phase transforms driven by entropy and defects to the h-(2×2) phase with hexagonal symmetry.

ACKNOWLEDGMENTS

Skillful technical assistance by W. Stiepany was instrumental for this study. One of us (P.M.-M.) acknowledges financial support of the Directorate-General for Science, Research and Development of the European Community.

* Present address: Université de Lausanne, Institut de Physique Expérimentale, CH-1015 Lausanne, Switzerland.
† Author to whom all correspondence should be addressed.

[1] D. Vanderbilt, Phys. Rev. B **36**, 6209 (1987).
[2] R. Feidenhans'l, J.S. Pedersen, J. Bohr, and M. Nielsen, Phys. Rev. B **38**, 9715 (1988).
[3] K. Takayanagi, Y. Tanishiro, M. Takahashi, and S. Takahashi, J. Vac. Sci. Technol. A **3**, 1502 (1985); Surf. Sci. **164**, 367 (1985).
[4] R.S. Becker, J.A. Golovchenko, and B.S. Swartzentruber, Phys. Rev. Lett. **54**, 2678 (1985).
[5] T. Ichikawa and S. Ino, Solid State Commun. **34**, 349 (1980).
[6] R.J. Phaneuf and M.B. Webb, Surf. Sci. **164**, 167 (1985).
[7] E.S. Hirschorn, D.S. Lin, F.M. Leibsle, A. Samsavar, and T.-C. Chiang, Phys. Rev. B **44**, 1403 (1991).
[8] R.M. Feenstra, A.J. Slavin, G.A. Held, and M.A. Lutz, Phys. Rev. Lett. **66**, 3257 (1991); Ultramicroscopy **42-44**, 33 (1992).
[9] I.-S. Hwang and J. Golovchenko, Science **258**, 1119 (1992); E. Ganz, S.K. Theiss, I.-S. Hwang, and J. Golovchenko, Phys. Rev. Lett. **68**, 1567 (1992).
[10] W.S. Yang and F. Jona, Solid State Commun. **42**, 49 (1982).
[11] M. Böhringer and J. Zegenhagen (unpublished).
[12] L. Seehofer and R.L. Johnson, Surf. Sci. **318**, 21 (1994).
[13] P. Molinàs-Mata and J. Zegenhagen, J. Phys. Condens. Matter **5**, 4687 (1993).
[14] Omicron Vakuumphysik GmbH, D-65232 Taunusstein.
[15] P. Molinàs-Mata *et al.*, Phys. Status Solidi A **148**, 191 (1995).
[16] P. Molinàs-Mata and J. Zegenhagen, Surf. Sci. **281**, 10 (1993).
[17] E. Artacho *et al.*, Phys. Rev. B **51**, 9952 (1995).
[18] M. Böhringer *et al.*, Phys. Rev. B **51**, 9965 (1995).
[19] J. Villain, Surf. Sci. **97**, 219 (1980); J. Phys. (Paris) Lett. **41**, L267 (1980).
[20] R.D. Meade and D. Vanderbilt, Phys. Rev. B **40**, 3905 (1989).
[21] N. Takeuchi, A. Selloni, and E. Tosatti, Surf. Sci. **307-309**, 755 (1994).
[22] Y. Sakamoto and J. Kanamori, Surf. Sci. **242**, 119 (1991); J. Phys. Soc. Jpn. **58**, 2083 (1989).

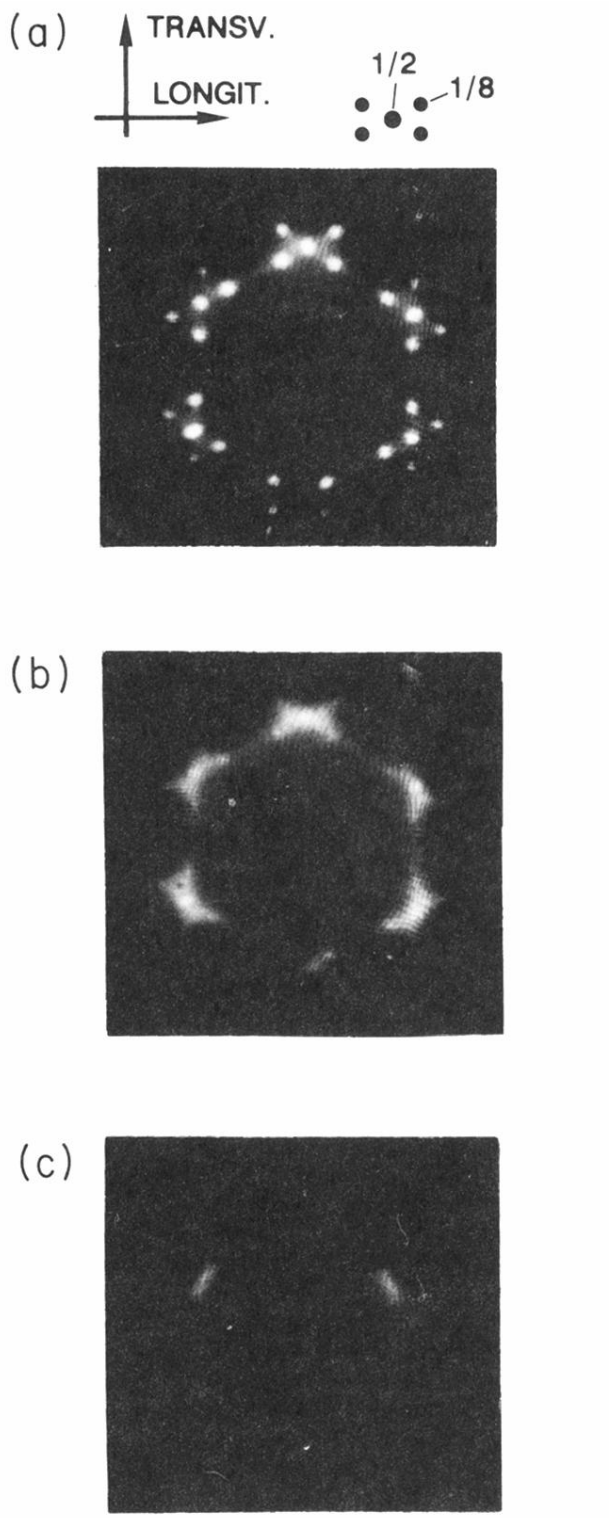

FIG. 1. (a) LEED photograph of the Ge(111)-$c(2 \times 8)$ surface (electron energy $E_0 = 17.0$ eV). (b) LEED photograph of the clean Ge(111) surface just below the transition to the $T > 300\,^{\circ}$C phase ($E_0 = 13.8$ eV). (c) LEED photograph of the Ge(111) surface just above the transition temperature to the $T > 300\,^{\circ}$C phase ($E_0 = 13.6$ eV). In (c) the temperature is ≈ 30 K higher than in (b). In all photographs only reflections around the 1/2-order positions are shown. The longitudinal (longit.) and transverse (transv.) directions are indicated.

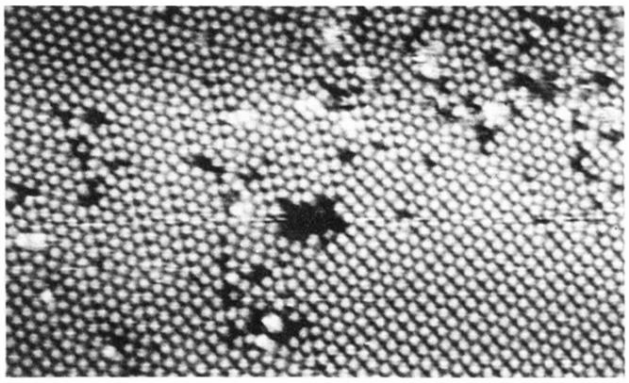

FIG. 11. STM image of a RT phase showing a striped (2×2) reconstruction in regions with low defect density (lower right) and a h-(2×2)-like reconstruction in regions with high defect density (left part). In this case, the defects are induced by small amounts of In, for which, however, we propose the same stabilization mechanism as for Ga (1.0 V, 50 pA, 350 Å $\times$ 220 Å).

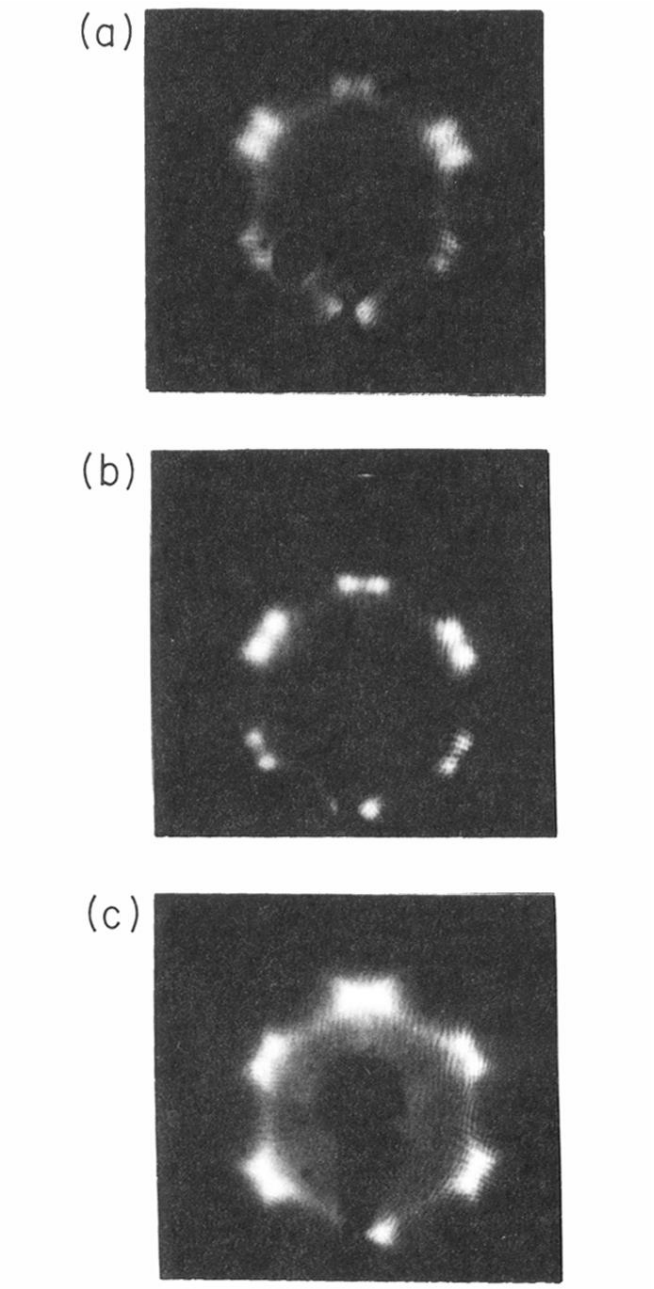

FIG. 2. (a) LEED picture of the Ga-induced RT phase with transversally elongated split 1/2-order reflections ($E_0 = 17.0$ eV). (b) LEED pattern of the Ga-induced RT phase with almost circular split 1/2-order reflections ($E_0 = 16.8$ eV). (c) LEED picture of a stabilized RT phase with intensity mainly between the 1/2-order and 1/8-order positions ($E_0 = 15.4$ eV).

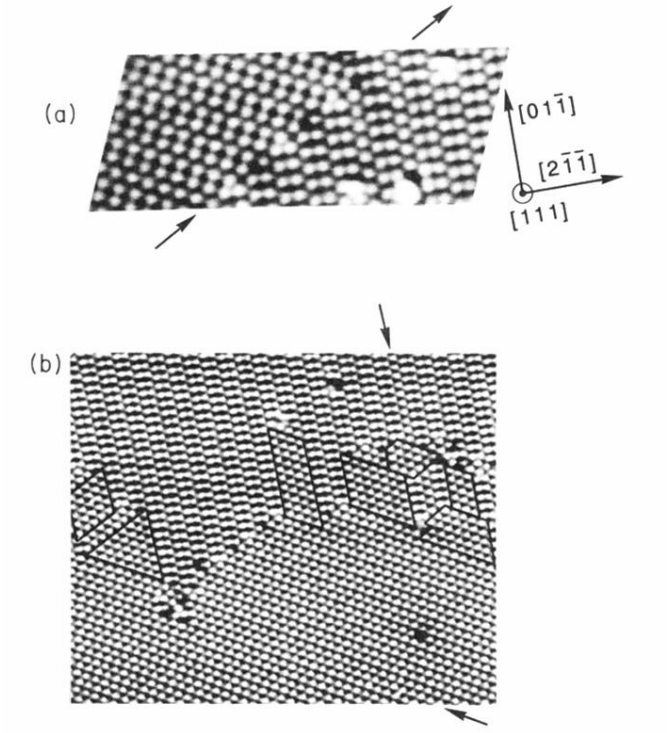

FIG. 3. (a) STM image of the Ge(111)-$c(2 \times 8)$ surface showing an "ideal" boundary between two $c(2 \times 8)$ domains (1.0 V, 50 pA, 180 Å $\times$ 70 Å). (b) STM image of the Ge(111)-$c(2 \times 8)$ surface showing locally (2×2) reconstructed areas (marked with a frame) and additional adatom rows along $\langle 01\bar{1} \rangle$ in local (2×2) geometry extending from the boundaries throughout the $c(2 \times 8)$ domains (marked by arrows) (1.0 V, 50 pA, 330 Å $\times$ 260 Å).

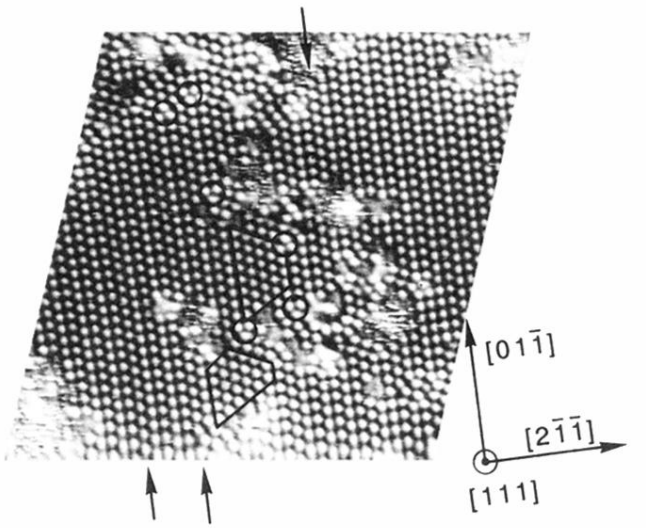

FIG. 4. STM image taken immediately after deposition of 0.05 ML Ga on a Ge(111)-$c(2\times8)$ surface at about 50 °C. Additional adatom rows (arrows), adatoms in local $(\sqrt{3}\times\sqrt{3})$ geometry (small circles), and (2×2) domains enclosed in $c(4\times2)$ walls (frames) are visible. The large defects with high corrugation are interpreted as Ga clusters (1.0 V, 50 pA, 300 Å × 300 Å).

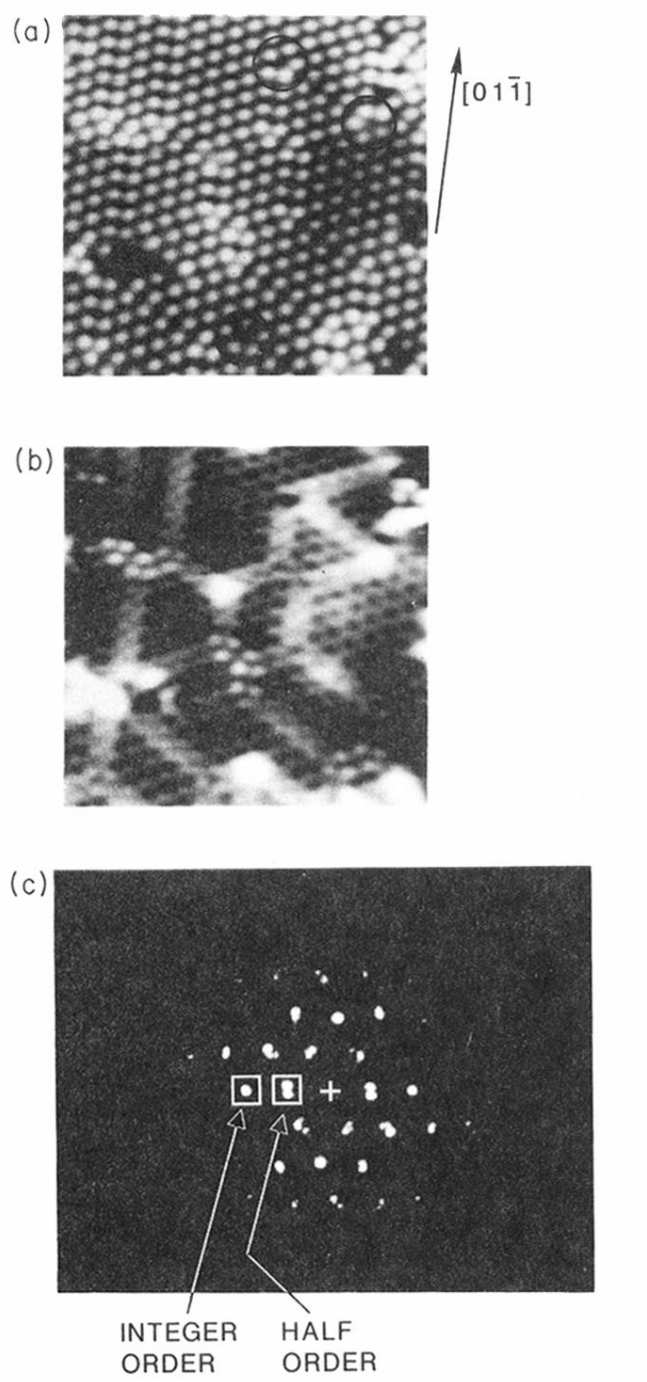

FIG. 5. DPI STM on the Ga-induced RT phase, showing close structural similarity with the h-(2×2) reconstruction: (a) $V_t = 0.6$ V, $I_t = 50$ pA, (b) $V_t = -0.6$ V, $I_g = 50$ pA (150 Å $\times$ 150 Å). (2×2) domains of adatoms are separated by $c(4 \times 2)$ walls with intersections in local $(\sqrt{3} \times \sqrt{3})$ geometry. At positive bias the adatom decoration of the surface is visible, while at negative bias the rest atoms also contribute to the observed corrugation pattern. At negative bias the quasi-hexagonal superstructure is clearly visible due to enhanced contrast at the walls [different charge transfer adatoms-rest atoms for $c(4 \times 2)$ and (2×2) units]. However, a deviation from the ideal h-(2×2) structure is caused by a high density of defects. The circles mark the "minimal" defects mentioned in the text. (c) Power spectrum of the Fourier transform of (a).

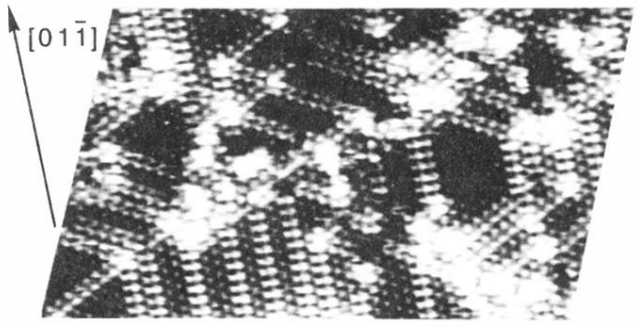

FIG. 6. STM image of a Ga-induced RT phase characterized in LEED [Fig. 2(c)] as transition between the $c(2 \times 8)$ and the h-(2×2) structures. Again, at negative bias the $c(4 \times 2)$ reconstructed walls appear higher than the (2×2) reconstructed stripes (-1.0 V, 50 pA, 330 Å $\times$ 330 Å).

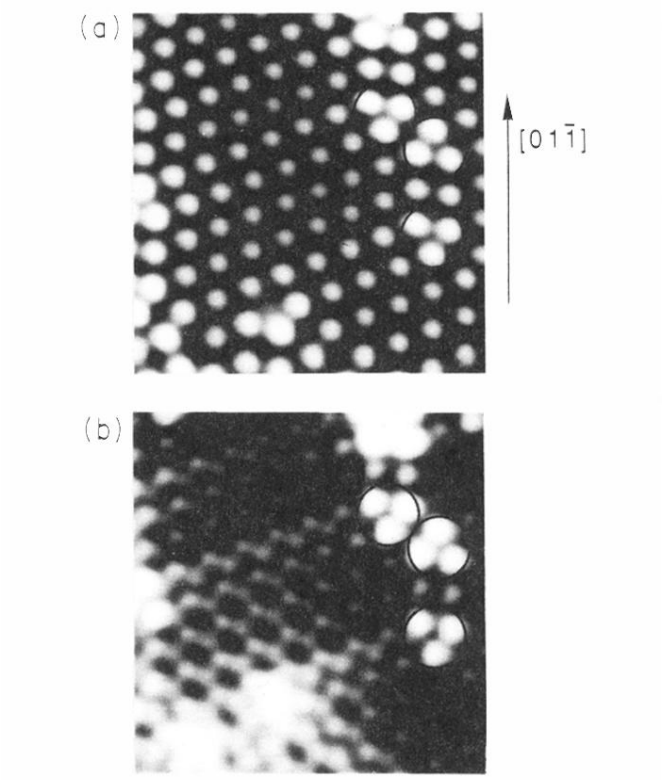

FIG. 8. DPI STM image of the Ga-stabilized phase showing the $(\sqrt{3} \times \sqrt{3})$ reconstructed domain wall intersections (circles) in more detail. (a) positive bias and (b) negative bias ($\pm$ 1.0 V, 50 pA, 80 Å $\times$ 80 Å).